Annual Report 2013

Institute of Engineering Geodesy (IIGS)

1. Members of Staff

Head of Institute:	Prof. Dr.-Ing. habil. Volker Schwieger	
Secretary:	Elke Rawe	
Emeritus:	Prof. Dr.-Ing. Dr.sc.techn.h.c. Dr.h.c. Klaus Linkwitz	
Scientific Staff:	Ashraf Abdallah, M.Sc.	GNSS Positioning
	Bara' Al-Mistarehi, M.Sc.	Construction Process
	Dr.-Ing. Alexander Beetz (until 30.11.2013)	Machine Guidance
	Shenghua Chen, M.Sc.	Kinematic Positioning
	Dipl.-Ing. Otto Lerke (since 01.10.2013)	Machine Guidance
	Xiaojing Lin, M.Sc.	Machine Guidance
	Dr.-Ing. Martin Metzner	Engineering Geodesy
	Dipl.-Ing. Annette Scheider	Kinematic Positioning
	Annette Schmitt, M.Sc. (since 01.04.2013)	Multi-Sensor-Systems
	Rainer Schützle, M.Sc.	Location Referencing
	Dipl.-Ing. Li Zhang	Monitoring
	Dipl.-Ing. Bimin Zheng	Monitoring
Technical Staff:	Martin Knihs Lars Plate Mathias Stange	
External Teaching Staff:	Dipl.-Ing. Christian Helfert	Fachdienstleiter Flurneuordnung im Landkreis Biberach
	Dipl.-Ing. Thomas Meyer	Landratsamt Ludwigsburg – Fachbereich Vermessung
	Dipl.-Math. Ulrich Völter	Geschäftsführer intermetric Gesellschaft für Ingenieurmessung und raumbezogene Informationssysteme mbH
	Dr.-Ing. Thomas Wiltschko	Entwicklungsingenieur Daimler Benz AG

2. General View

The Institute of Engineering Geodesy (IIGS) is directed by Prof. Dr.-Ing. habil. Volker Schwieger. It is part of the Faculty 6 "Aerospace Engineering and Geodesy" within the University of Stuttgart. Prof. Schwieger holds the chair in "Engineering Geodesy and Geodetic Measurements". In 2012 he was elected as Vice Dean of the Faculty 6.

In addition to being a member of Faculty 6, Prof. Schwieger is co-opted to the Faculty 2 “Civil and Environmental Engineering”. Furthermore, IIGS is involved in the Center for Transportation Research of the University of Stuttgart (FOVUS). Prof. Schwieger presently acts as speaker of FOVUS. So, IIGS actively continues the close collaboration with all institutes of the transportation field, especially with those belonging to Faculty 2.

Since 2011 he is full member of the German Geodetic Commission (Deutsche Geodätische Kommission – DGK). Furthermore, Prof. Schwieger is a member of the section „Engineering Geodesy“ within the DGK. He is head of the DVW working group 3 “Measurement Techniques and Systems” and chairman of the FIG working group 5.4 “Kinematic Measurements”.

The institute’s main tasks in education focus on geodetic and industrial measurement techniques, kinematic positioning and multi-sensor systems, statistics and error theory, engineering geodesy and monitoring, GIS-based data acquisition, and transport telematics. Here, the institute is responsible for the above-mentioned fields within the curricula of “Geodesy and Geoinformatics” (currently Diploma, Master and Bachelor courses of study) as well as for “GEOENGINE“ (Master for Geomatics Engineering in English language). In addition, the IIGS provides several courses in German language for the curricula of “Aerospace Engineering” (Master), “Civil Engineering” (Bachelor and Master), “Transport Engineering” (Bachelor) and “Technique and Economy of Real Estate” (Bachelor). Furthermore, lectures are given in English to students within the master course “Infrastructure Planning”. Finally, eLearning modules are applied in different curricula. Also during the year 2013, teaching was still characterized by the conversion of courses from Diploma to Bachelor and Master degree, now with the focus on the Master degree. This is going to continue within the next year.

The current research and project work of the institute is expressed in the course contents, thus always presenting the actual state-of-the-art to the students. As a benefit of this, student research projects and theses are often effected in close cooperation with the industry and external research partners. The main research focuses on kinematic and static positioning, analysis of engineering surveying processes and construction processes, machine guidance, monitoring, transport and aviation telematics, process and quality modeling. The daily work is characterized by intensive cooperation with other engineering disciplines, especially with traffic engineering, civil engineering, archotecture and aerospace engineering.

3. Research and Development

3.1. Center for Transportation Research University of Stuttgart (FOVUS)

In 2013, the main activity within FOVUS was to prepare and submit research proposals on a national and an international level. A cooperation between German Rail (Deutsche Bahn AG) and University of Stuttgart was prepared mainly by the members of FOVUS.
With respect to education, the re-organization of the transportation-related study programs at the University of Stuttgart has been successfully completed. In the winter term 2013/2014, the second set of students enrolled for the new study program “Transportation Engineering”, in which also the IIGS is involved.

3.2. Location Referencing

Today, a number of devices, applications, and services gather, receive, share, visualize, or generally speaking, process information that somehow has a location-component. In many applications, this location-based information is referenced to objects in an electronic map (e.g. roads, buildings, etc.). The application areas range from smartphone apps to find the next restaurant or cash machine to safety-relevant vehicle-based systems with high requirements to reliability and robustness.

Two kinds of such map-based applications can be distinguish. The first category uses only one map base and all exchanged objects are referenced to this map. This can be achieved, with mobile clients (e.g. Smartphones, vehicle-based systems) using the same application, which is connected to a central map server. The objects are denominated by their object ID and can be uniquely identified within that closed system. A second kind of applications is open to be used with different types of clients with different maps in use. Such systems have the chance to reach a higher dissemination as client systems are not restricted to specific applications and vendors. One drawback, however, needs to be dealt with: map objects cannot be uniquely identified among different maps. A different and more generalized way to express the location of an information object is needed. Such systems are called “Location Referencing” systems and enable the exchange of information objects between different systems using different maps.

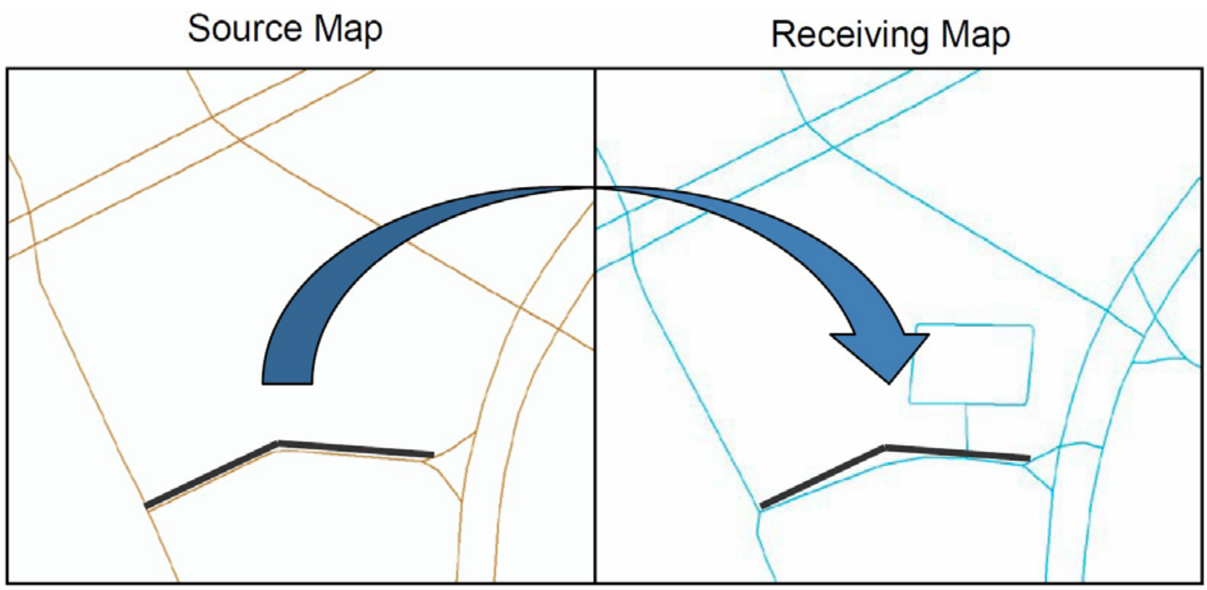

Fig. 1: Transferring a location reference

A location must be defined on the source map as a set of line elements on that map. The encoder then collects all required information about this location from the source map and wraps it altogether into the “location reference”. This location reference is being transmitted to the receiving system using a (probably) different kind of road map. In this system, a decoder unwraps the received location reference and searches its map for the corresponding lines that cover the same route as the original location on the source map (Figure 1).

The location reference contains information about the geometric, topologic and semantic (i.e. attributes like road names and road class) properties of the original location. The transmitted information, however, has to satisfy a number of constraints:

The bandwidth of the communication carrier (normally mobile internet connection) is limited. Furthermore, especially the transmitted semantic information cannot be matched without having a proper attribute mapping due to different attribute schemas at the different maps.

Available methods, like AGORA-C or OpenLR, have been used in different research projects in the past, however only reached moderate or even poor results. For some recent commercial applications of location referencing methods, the systems were restricted to specific maps which also were optimized for this particular use-case. Moreover, the location referencing data exchange format had to be adapted to the special circumstances. Altogether, the final system worked quite well but was restricted to a specific use-case, specific clients, and was not an open and flexible system anymore.

For the purpose of testing the possibilities of enhancing the success rate of such dynamic and map-agnostic location referencing systems, the IIGS sets up a location referencing test bed. During the reporting period, this test bed has reached a first intermediate functional level. It is capable of en- and decoding locations on different maps provided in shape file format. Maps that do not satisfy the format specifications directly, as for example from OpenStreetMap, can be converted using a specifically developed map converter. Batches of locations can be processed at once, the result sets are stored in a defined way and can be visualized for manual inspection together with their underlying maps in ArcGIS quite handily using a newly developed Python-tool. Automatic evaluation procedures are capable to identify locations that might not have passed the transfer from one map to the other without fault. These locations can be inspected manually to identify possible possibilities for improvement in the location referencing procedures.

3.3. Time-Spatial Analysis for Low-Cost GPS Time Series

Multipath effects are the dominating errors for short baselines in monitoring applications. The time and spatial correlation can be analyzed by applying closely-spaced antennas. Three low-cost antennas with low-cost receivers have measured on the roof of the IIGS building. The three antennas were arranged in two positions: orthogonal (position 1) and parallel (position 2) to the wall (compare fig 2). It is expected that the multipath effect changes much more in position 1 than that in position 2.

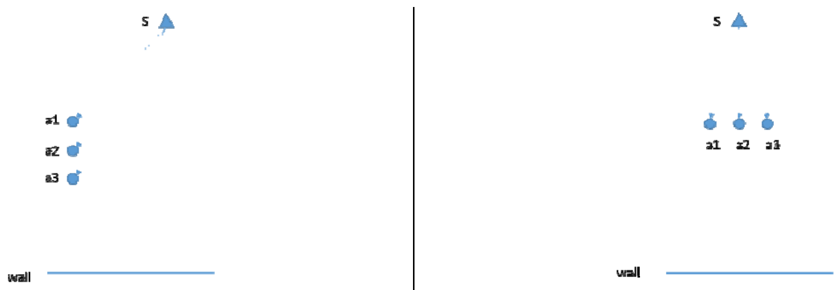

position 1 (orthogonal to wall) position 2 (parallel to wall)

Fig. 2: Two test constellations (not scaled)

The distance between two adjoining antennas is 50 centimeters, the three antennas are numbered as a1, a2 and a3. The distance between the a2 (the middle one) and the wall is about 4.2 meters in position 1 and about 5.1 meters in position 2 and the antenna heights are all about 1.2 meters. The SAPOS station in about 500 meters

away was taken as reference station and the three low-cost antennas as rover stations for the baselines. The GPS raw data (UBX-format) were stored directly from u-blox EVK-6T receivers with 1 Hz sampling rate. The receivers were measured in each position for several days.
The processing results are baselines (coordinates' differences) in UTM for every second. The time series of the coordinates were analyzed, about 5% outliers were detected and interpolated. There are no significant linear and short periodic trends (besides the period of one sidereal day) which can be found.
The cross-correlation between the baselines can be calculated. One simple approach was applied to improve the accuracies by using these spatial cross-correlations. It is assumed that the error influences are similar for each antenna; they change linear in space. For example, the coordinate of antenna 2 can be corrected by the coordinates of antenna 1 and 3 by considering the cross-correlation. It can be calculated as blow:

$$x_{2\_cor}(t) = x_2(t) - \frac{K_{12}}{K_{12}+K_{23}} \cdot x_1(t) - \frac{K_{23}}{K_{12}+K_{23}} \cdot x_3(t)$$

The $x_1(t)$ to $x_3(t)$ on the right side are the original coordinates' residuals in east, north and height components. K_{12} and K_{23} are the correlation between the baselines s-a1 and s-a2, and between s-a2 and s-a3. They depend on the duration of the observations and on the positions. For testing this approach, one day solutions and four hour solutions were taken for each position.
Table 1 and 2 show the original and improved standard deviations of baseline s-a2 by applying the approach. Generally, almost all the standard deviations were improved (only one exception marked in table 2). The percentage of improvement is very different (maximum is 46%), on average about 21% for position 1 and 25% for position 2.

Table 1: Original and Improved Standard Deviation of Baseline s-a2 (Position 1)

Position 1	Original standard deviation [mm]			Improved standard deviation [mm]		
s-a2	E	N	h	E	N	h
One Day solution	3.3	6.2	9.4	3.0	5.4	8.2
1. hour	1.9	4.1	5.4	1.7	2.5	5.1
2. hour	3.7	16.6	10.0	2.8	13.2	7.5
3. hour	2.7	5.3	16.6	1.5	3.5	10.6
4. hour	4.0	5.5	8.4	3.6	4.1	7.3

Table 2: Original and Improved Standard Deviation of Baseline s-a2 (Position 2)

Position 2	Original standard deviation [mm]			Improved standard deviation [mm]		
s-a2	E	N	h	E	N	h
One Day solution	3.3	5.7	9.5	2.3	4.1	7.0
1. hour	2.0	3.2	5.8	1.4	1.9	5.9
2. hour	2.5	3.1	5.8	2.2	2.0	5.6
3. hour	2.1	3.0	5.9	1.5	1.7	4.3
4. hour	2.4	3.3	10.7	2.0	2.1	7.3

From these first test results, it can be seen that the approach that takes the spatial correlations into account can improve the accuracies of the results. The linear combination of correction is the simplest assumption. In the future, the spatial correction should be analyzed in more detail and another better and more reliable approaches can be developed.

3.4. Precise Point Positioning (PPP) using Bernese Software

The Bernese GNSS software Version 5.2 (BSW5.2) is scientific, high-precision processing software which was developed by the Astronomical Institute of the University of Bern (AIUB). Using Bernese software In PPP processing, the satellite orbits and clock data are available from the Center for Orbit Determination in Europe. The satellite and receiver phase center data is provided by IGS ANTEX standard data. For tropospheric modelling there are many models available in the software for dry and wet tropospheric parts. Moreover, the gradient models and mapping functions are also offered. The second order of ionospheric delay and high ionospheric orders are estimated in the PPP processing. Additionally, there are many other highly accurate models in the algorithms (e.g. ocean loading, atmospheric tidal loading).

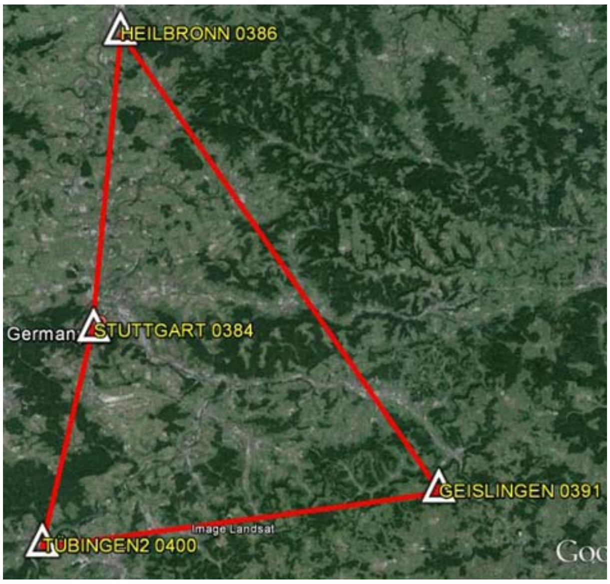

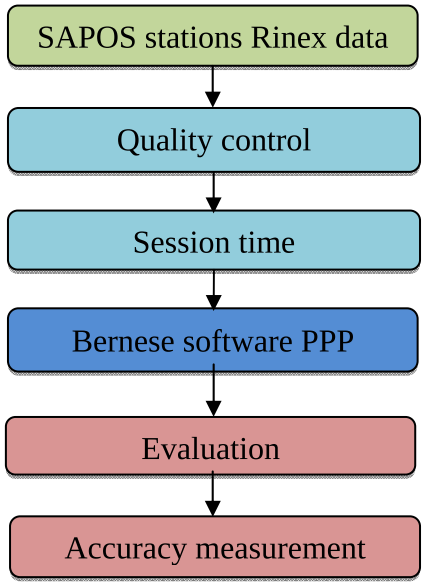

Fig. 3: SAPOS's Stations layout (left) - Processing procedure for PPP solution (right)

To evaluate the PPP processing technique using Bernese software, four SAPOS stations (Stuttgart, Tübingen2, Geislingen and Heilbronn) with 24 hours observation time and 30 seconds sample interval were processed for static and kinematic techniques, (see Figure 3, left). The antenna type is TRM59800.00 SCIS and receiver type is TRIMBLE NETR5. Figure 3 (right) shows the processing procedure in static and kinematic technique. Bernese software provides the possibility to detect the session time or the observation time. The data is checked using teqc software before processing. In this processing, the observation time of the four stations were divided from 1 hour up to 24 hours. The error values are computed between the reference solution and the PPP solution.

In case of static-PPP technique; Figure 4a illustrates the error in horizontal direction (position) for the four stations with different convergence times. The position error after 4 hours is around 1 cm and reaches mm after 12 hours. Figure 4b shows the error in height direction for the four stations in cm. The height error after 4 hours is around 2 cm and reaches 1 cm after 12 hours of convergence time for three of the four stations.

In case of kinematic-PPP technique; Figure 5a shows the RMS error in position for the different stations. For stations 0384, 0386 and 0400; the RMS error value reaches the level of 2 cm for 4 hours observation time. This error value is nearly stable to the end of this processing. Another side; station 0391 provides an RMS error in 2D of more than 2 cm for some observations times. The height RMS error is depicted in Figure 5b. The RMS error value is in between 2 to 5 cm after 4 hours. This error value reaches 2 to 3 cm after 12 hours.
The processing using Bernese software will be continued for the real kinematic tracks to assess the accuracy of PPP technique.

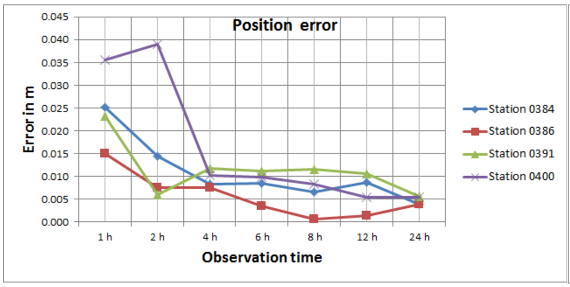

Figure 4a: Position error values for all stations in m for static-PPP

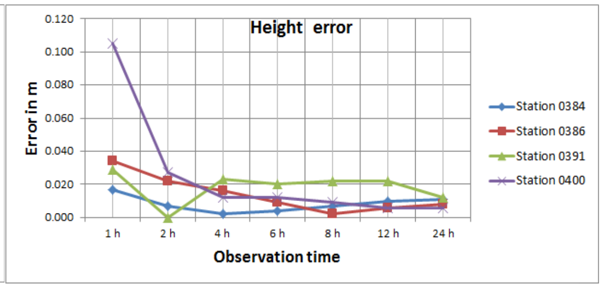

Figure 4b: Height error values for all stations in m for static-PPP

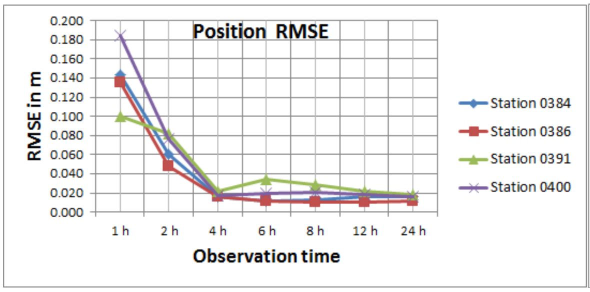

Figure 5a: Position RMSE values for all stations in m for kinematic-PPP

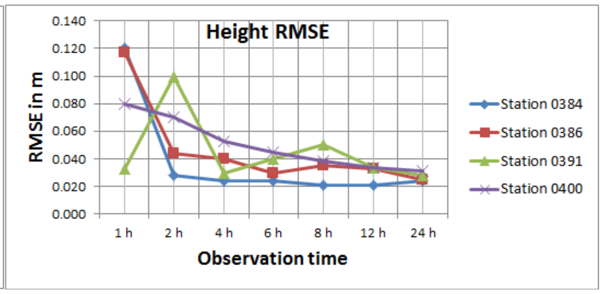

Figure 5b: Height RMSE values for all stations in m for kinematic-PPP

3.5. Further Development of the Construction Machine Simulator

The institute spent several years in developing a construction machine simulator. Now, GNSS-RTK solutions are integrated for the out-door simulator. A concrete plate was constructed for carrying out the outdoor simulator tests on Vaihingen Campus, University of Stuttgart. It is shown in the Figure 6. There are four pillars around the plate as a control network and the coordinates of the pillars are determined with GNSS static observation data and terrestrial measurements. According to the stake out data from the engineering construction map, the reference trajectory is generated on this plate. Different drive tests are carried out to investigate the control quality of the RTK solution.
The RTK-solution is computed using GNSS-Receivers of Leica Geosystems combined with SAPOS. The hardware components for the guidance system and their interactions are shown in Figure 7. The GNSS antenna is installed in the geometric center of the model truck. The model truck is composed of a steering servo-motor, a velocity motor and a receiver to obtain voltage from the remote controller. The Leica GNSS receiver provides real-time 3D positions to the computer using radio modems. The control program which is developed with the programming language Labview computes the lateral deviation between the measurements and the reference trajec-

tory. The digital-analogue converter converts the steering angle to voltage and sends it to the remote control.

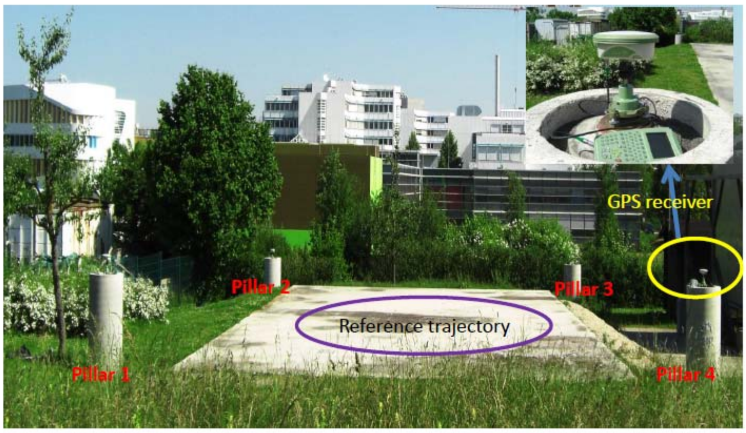

Fig. 6: Test field of the out-door simulator

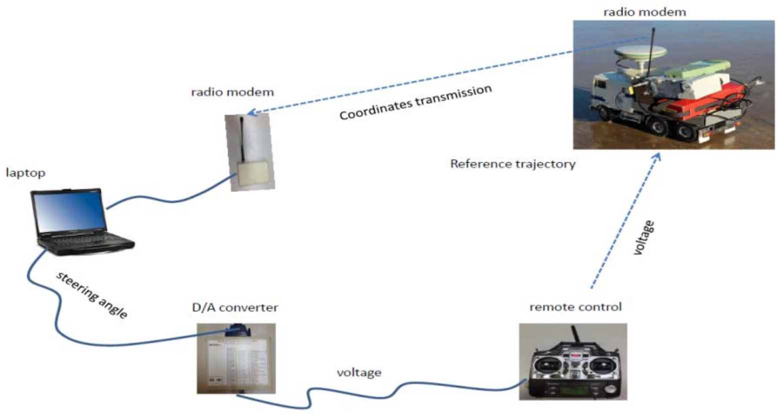

Fig. 7: Hardware components of the simulator

The experimental results show that the RMS of the lateral deviation is about 8-12 mm for a velocity of 7 cm/s with the 5 Hz real-time RTK solution. If the observation data is 20Hz, the RMS of the lateral deviation is about 5-8 mm for a velocity of 7 cm/s and 14 cm/s. The PID controller works better than the P, PI and PD controllers with different velocities and different observation data rates. The impact of the Kalman filter on the RMS of the lateral deviation is not significant when the velocity of the truck is about 7 cm/s and 14 cm/s. However, when the truck drives with a velocity of 30 cm/s, the control quality is improved by 1.6 mm by the implementation of the Kalman filter.

3.6. HydrOs - Optimization of Positioning in Areas of GNSS Shadowing along Inland Waterways

German inland waterways are surveyed by surveying vessels e.g. with multibeam depth sounders. The measured profiles of the river bed must be georeferenced, so the position of the vessel and the depth sounder respectively must be known. Currently many surveying vessels are equipped with GNSS antennas to determine their position. But positions in GNSS shadowed areas, e.g. under bridges or close to riparian vegetation, cannot be determined. Currently, these positions are calculated with a linear interpolation between known positions in post-processing mode.

The project HydrOs aims to developing an integrated hydrographic positioning system in cooperation with the German Federal Institute of Hydrology (BfG) to avoid cost-effective post-processing procedures. A multi-sensor system is designed, so multiple sensors can be used to determine the position of the vessel, if it is not possible to receive the GNSS signals. Next to GNSS, a GNSS-INS coupled system is already available on the vessels used for the HydrOs project. Additionally a Doppler Velocity Log (DVL), barometer, wind sensor and ampere meters to obtain the propeller directions and their revolution speed are integrated into the system. The HydrOs software already records the measured data. Besides, a filter module to process the data in real-time mode is currently developed.

Because of the non-linear model and observation equations an Extended Kalman Filter (EKF) is used for the evaluation of the measurements.

The developed motion models predict the following state variables in three dimensions: Angular rates, velocity components, orientation angles and coordinates. The angular rates and the orientation angles are always predicted with the same algorithm, but there are different approaches for the velocity components and the coordinates (Fig. 8). One model approach predicts the position change between epoch *k* and epoch *k+1* linearly referred to the coordinate axes of the local ship coordinate system. The spherical approach describes the coordinate changes on a great circle with curve radius *R*. To adapt the prediction quickly to driving manoeuvres, regulating variables are inserted into the model. For that purpose, also two approaches are evaluated: The resulting propeller direction as single regulating variable or a vector of regulating variables containing direction and rotation frequency of the propellers, flow velocity components, speed and direction changes caused by wind influence.

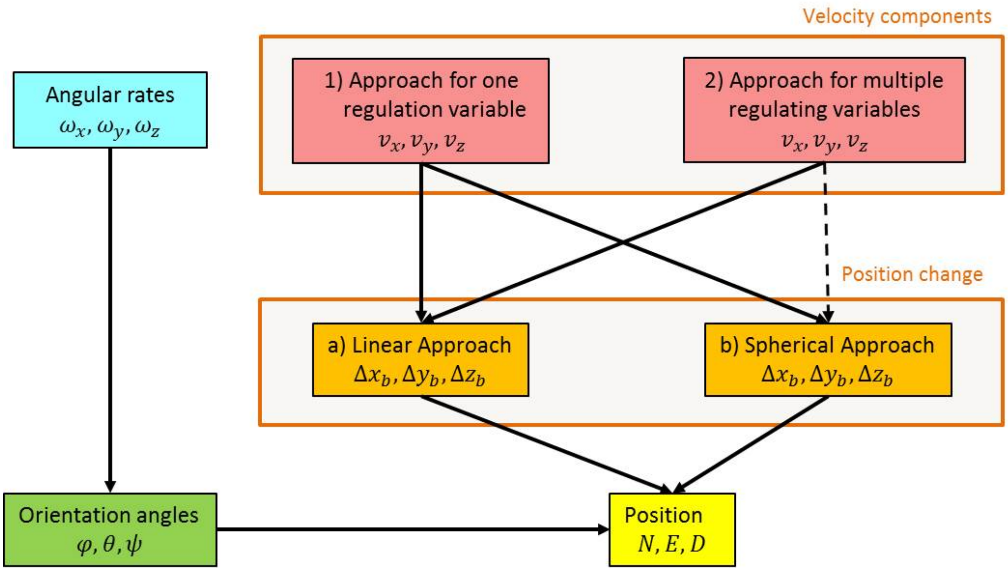

Fig. 8: Simulation scenarios

A performance test of the developed models was conducted using the Monte Carlo method. Therefore, measurement signals were simulated for a straight drive and a drive along a curve. For full observations availability it is shown that the described models reach an adequate accuracy level within the EKF. Because the regulating variables caused by wind are assumed to reach only a medium accuracy level, the approach for one resulting variable seems to be more promising. If a GNSS signal gap of 60s is simulated, the requirements are fulfilled for more than 90% of all cases provided that the linear approach with one regulating variable is used. But this means that the models must be improved furthermore to increase the reliability of the system.

For this reason, it is also important to detect GNSS measurements within regions of restricted GNSS signal reception. If they do not fulfill the requirements concerning position accuracy, those observations must not be integrated to the EKF. Therefore investigations have been conducted with multiple GNSS antennas on a platform. Some criteria were determined which might be used to detect inaccurate GNSS observations. The most promising solution combines several parameters like DOP values and the difference of measured velocities for different GNSS antennas.

Another sensor which was investigated concerning its ability of being integrated into the multi-sensor system was barometer. The measured air pressure was transferred to absolute and relative heights, so that the deviations could be considered. Only short-time height differences can reach an accuracy level of a few decimeters, other kinds of barometric height determinations are not accurate enough.

3.7. Detection of Hydrothermal Deformations of Sandstone using Laser Scanning

The damage documentation of cultural heritage, like buildings or sculptures, poses a great challenge to conventional measuring techniques. The main building of the University of Applied Sciences Stuttgart (HfT) was built from 1867 to 1873. The façade consists of sandstone, which is the most popular construction material for the historical city architecture in Baden-Württemberg. For our research two areas of the façade were chosen, in which there are at least 4 different types of damage like alveolarisation, crack, detachment, graffiti and algae. Each area is around 2x2 m² (Figure 9).

Fig. 9: Two areas on the façade (Area 1: left, Area 2: right)

It was planned to scan both areas in 6 different epochs. The first measurement took place on 22nd Feb. 2013. Epoch 2 was chosen as reference for the deformation analysis. For the deformation analysis of area 2, only the measurements from epoch 2,3,4,5 were used. Area 2 was not scanned in Epoch 6 because of a tree showing leaves for the first time in front of the façade.
Before carrying out the deformation analysis, the point clouds must be pre-processed in several steps (Figure 10). In Leica Cyclone all point clouds were georeferenced in the local coordinate system. For deformation analysis the exact border and the sizes of all epoch scans were defined and calculated in Matlab. In order to calculate and describe the deformation between two different epochs, the local normal vectors and the local volume changes were chosen for the comparison. After “façade cutting” the changes of the local normal vectors and of the volume were also calculated in Matlab. Then the classifications of both comparisons were visualized. Finally the statistical tests were carried out for the deformation analysis.

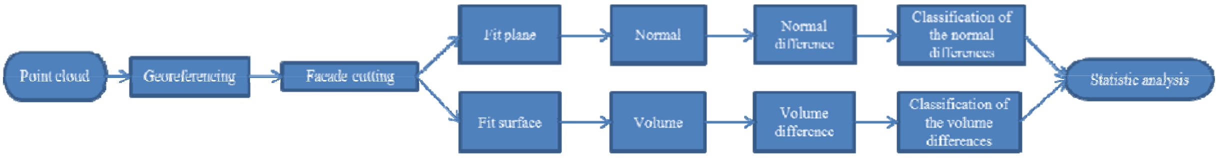

Fig. 10: Flow diagram of the data analysis

The difference vectors and their absolute values were calculated. With respect to the angle in radiant between normal vector $\mathrm{n_{i\_epoch2}}$ of grid i in epoch 2 and the normal vector $\mathrm{n_{i\_epochj}}$ of grid i in epoch j the grids were colourised. With respect to the change of the volume, the grids were colourised, too (Figure 11). The change of the volumes is strongly correlated with changes in air temperature.

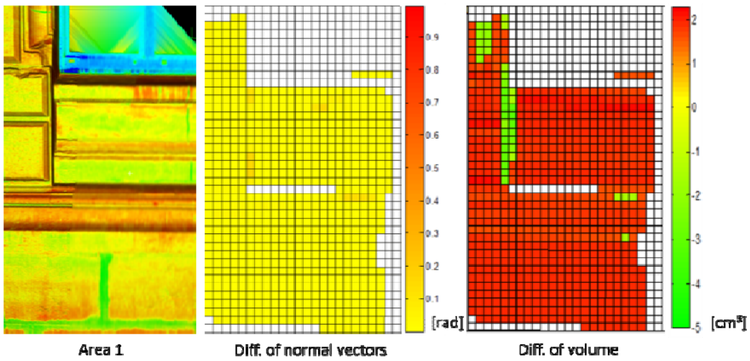

Fig. 11: Comparisons of area 1 between epoch 2 and epoch 3

The maximum angle difference of 0.95 rad between two normal vectors is calculated for the comparison of epochs 2 and 5 in area 1. Particularly with regard to the change in temperature it can be seen that the normal vectors with big differences are concentrated in the edge-area near the window. One possible supposition is that the air exchange may have an influence on this area, if the connection area between façade and window is not well isolated. Besides, the grids with big angle differences are located mainly at edge structures. In such areas the noise of the point clouds is strong and the number of points is reduced. The second reduces the redundancy of the plane estimation. Most of the angles are in intervals between 0 rad and 0.3 rad. The maximum volume difference -5.1 cm³ can be found in area 1 between epoch 2 and 5. The volume differences as well as the angle differences of the normal vectors have to be tested with respect to their significance. For both cases normal distributed values and a significance level of α=0.05 were assumed. Not all differences are significant. A typical pattern cannot be recognized from the data.

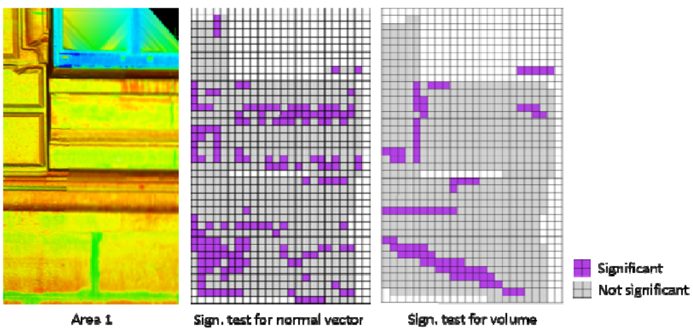

Fig. 12: Significance tests for nomal vector and volume changes of area 1

If figure 12 is observed, patterns are visible that cannot be explained. At the present it is not possible to give a complete explanation. It can be stated, however, that the standard deviation of the volume is strongly correlated with the standard deviation of the surface parameters. Take the grid 421 and 422 from area 1 in epoch 3 as an example (Figure 13).

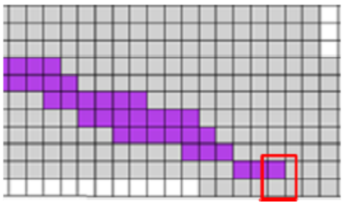

Fig. 13: Example for the significance test

Grid 422 has a volume difference of -5.7 cm³, which has the same magnitude like the volume difference of -5.3 cm³ of grid 421. The volume difference of grid 421 is significant, unlike the one of grid 422 (Table 3). This is caused by the respective standard deviations and finally by the standard deviations of the polynomial parameters: 0.002 in grid 422 is worse than 0.0005 in grid 421. This means that the surface fitting function has to be investigated in more detail in the future.

Grid	ΔV [cm³]	σ_ΔV [cm³]	σ_P
421	-5.3	2.6	0.0005
422	-5.7	5.9	0.002

Table 3: Accuracy of volume difference

In the next step the correlation between the surface parameters and the volume accuracy must be analysed. In the future, continuous temperature and huminity measurements nearby the façade have to be realized to overcome the deficiency. One approach to be considered in the modelling of the temperature and humidity influences by a finite element model (FEM) of the sandstone façade or in any case a part of it. In the best case the calibration of this model using geodetic measurements can be the target.

3.8. Automated Detection for Cracks Detection

Crack detection is considered as one of the most important issues in transportation and highway engineering. In the past, conventional visual and manual pavement distress analysis approaches were very costly. Also the measuring of linear cracks is consuming a lot of time, it is dangerous, labor-intensive, tedious, and subjective. For these reasons several image processing methods for crack detection algorithms have been developed. But many of them which depend on approximation algorithms, face some obstacles and problems. The work of this year provides an automated image processing crack detection algorithm. The goal is to extract automatically the linear cracks from sequence pavement images of different streets in Germany. The sequence pavement images (mobile mapping data) were observed by two Germany companies as follows: *LEHMANN + PARTNER GmbH* company using S.T.I.E.R mobile mapper system and *3D Mapping Solutions GmbH* company using MoSES mobile road mapping system.

Different case studies with different lighting conditions were analysed to evaluate the proposed automated image processing crack detection algorithm technique. Figure 14 illustrates the processing and evaluation methodology for crack detection. The proposed automated crack detection algorithm provides the possibility to detect the linear cracks from sequence pavement images (mobile mapping data) with different lighting conditions. Also the speed up factor shows a significant improvement.

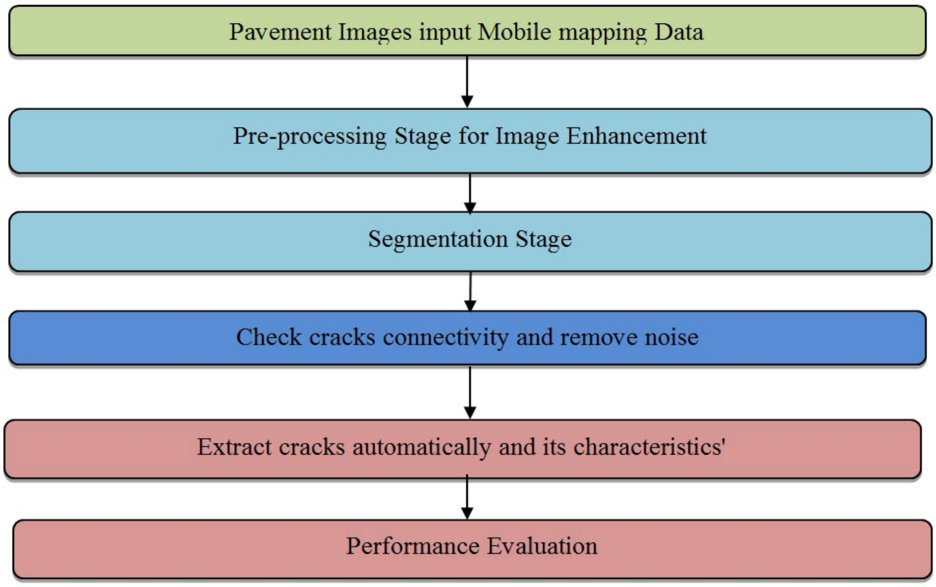

Fig. 14: The processing and evaluation methodology for crack detection

3.9. Robotics in Timber Construction

The project *Robotic Fabrication in Timber Construction* is realized in co-operation with the Institute for Computional Design, the Institute of Building Structures and Structural Design, industrial partners and partners from the state Baden-Württemberg. The goal of this project is to combine robotic fabrication with computational design, simulation processes, and 3D-surveying.

The result of this project will be a demonstrator pavilion, shown in Figure 15, for the state horticultural show *Landesgartenschau 2014* in Schwäbisch Gmünd. The pavilion will be constructed of 243 wooden elements which will have been produced by industrial robots. The elements, which consist of plywood with a thickness of 50 millimeters, are preformatted by a CNC-machine and afterwards processed by the robots.

Fig. 15: Pavilion

The surveyor's part in this project is the quality control of the elements and, after having built up the pavilion, the deformation analysis using laser scanning data. The quality control is effected by the laser tracker. The results of the laser tracker measurements are compared to the given design model.
For the quality control of the elements, a laser tracker API Radian is used together with the API IntelliProbe360™. The quality control is carried out by a control sample, this means that out of 243 elements 24 are measured. To measure the edges of the element a special adapter for the IntelliProbe360™ is developed by IIGS. As shown in Figure 16, each has at least five edges with minimum one box joint.

Fig. 16: Wooden Element

On each element of the box joint at least five points were measured. These pointwise measurings are compared with the CAD model. This comparison is effected by Spatial Analyzer's function "*Relationships*", which calculates the minimum distance between the measured point and the edges of the CAD model. The average aberration is 0.97 mm for all measured elements.
Wood is a vital basic material, for that reason four elements will be measure three times. So the change between the moment after production, shortly before transportation and after one night at the building site can be shown.

The next step will be the deformation analysis of the pavilion, which will be performed by a laser scanner. There will be a detailed investigation of the four elements which were measured three times by the laser tracker.

4. Publications

Beetz, A, Schwieger, V.: Automatic lateral control of a model dozer. Journal of Applied Geodesy, Heft 4, de Gruyter, 2013

Cramer, M., Schwieger, V., Fritsch, D., Keller, W., Kleusberg, A., Sneeuw, N.: Geoengine – the university of Stuttgart International master program with more than 6 years of experience. FIG Working Week, Abuja, Nigeria, 06.-10.05.2013 and Interexpo Geo-Siberia, Novosibirsk, Russia, 24.-26.04.2013.

Kealy, A., Retscher, G., Schwieger, V.: Preface to the Special Edition of the JAG on Ubiquitous Positioning and Navigation Systems. Journal of Applied Geodesy, Heft 4, de Gruyter, 2013.

Kuhlmann, H., Schwieger, V., Wieser, A., Niemeier, W.: Ingenieurgeodäsie – Definition, Kernkompetenzen und Alleinstellungsmerkmale. Zeitschrift für Vermessungswesen, Heft 6, Wißner Verlag, 2013.

Scheider, A., Schwieger, V.: Entwicklung von Verfahren zur Verbesserung der Ortung mit Global Navigation Satellite Systems (GNSS). BfG-Kolloquium: Neue Entwicklungen in der Gewässervermessung, Koblenz, 20./21.11.2012.

Schwieger, V., Lilje, M.: Innovative and Cost-effective spatial positioning. FIG Working Week, Abuja, Nigeria, 06.-10.05.2013 and Interexpo Geo-Siberia, Novosibirsk, Russia, 24.-26.04.2013.

Schwieger, V., Schweitzer, J., Zhang, L.: Ingenieurgeodästische Qualitätsmodllierung im Bauprozess. In: 125. DVW-Seminar: Qualitätssicherung geodätischer Mess- und Auswerteverfahren. Hannover, 24.-25.06.2013.

Zhang, L., Schwieger, V.: Investigation regarding different antennas combined with low-Cost receiver. FIG Working Week, Abuja, Nigeria, 06.-10.05.2013.

Zhang, L., Schwieger, V.: Monitoring mit Low-Cost GPS Empfängern – Chancen und Grenzen. In: 124. DVW-Seminar: GNSS 2013 – Schneller, Genauer, Effizienter. Karlsruhe, 14.-15.03.2013.

Zheng, B., Schwieger, V., Grassegger-Schön, G.: Detection of hydrothermal deformations of sandstone using laser scanning. 2nd Joint Symposium on Deformation Monitoring, Nottingham, UK, 09.-10.09.2013.

5. Presentations

Schwieger, V.: Construction Machine Guidance. Technical University of Construction Bucharest, Rumania, 18.-22.11.2013.

Schwieger, V.: Low Cost GNSS. Technical University of Construction Bucharest, Rumania, 18.-22.11.2013.

Schwieger, V.: Multi Sensor Systems. Technical University of Construction Bucharest, Rumania, 18.-22.11.2013.

Schwieger, V.: Trajektorienbestimmung mittels Kalman Filter. 10. Jenaer GeoMessdiskurs. 01.07.2013.

Zhang, L.: Monitoring mit Low-Cost GPS Empfängern – Chancen und Grenzen. In GNSS 2013 – Schneller. Genauer. Effizienter. 124. DVW-Seminar am 14. und 15. März 2013 in Karlsruhe.

6. Diploma Theses and Master Theses

Alhessi, Mohammed: Development and Implementation of an OpenLR Map Interface for Shape-Files.

Anisia, Vlad-Daniel: Comparison of two Software Products for the Object Modelling with Respect to Deformation Analysis using FARO Focus 3D Data.

Fitz, Daniel: Bestimmung von Referenz-Positionen für die photogrammetrische Auswertung von UAV-Bildflügen mittels einer automatischen Totalstation.

Ren, Zhenjie: Design, Implementation and Evaluation of Sensor Concepts for Robot Localization in the Indoor Area.

Wei, Xingyu: Analysis of Damage Dynamics on the North-East *Facade* of the HFT Stuttgart using Leica Laser- Scanner HDS7000.

Wen, Xinda: Development of Evaluation Functions for a Collosion Measuring Stand

7. Study Theses and Bachelor Theses

Bosch, Jascha: Untersuchung der Positionsgenauigkeit kinematischer GNSS Messungen in teilabgeschatteten Bereichen.

Diemer, Luis: Entwicklung eines formbasierten Location Referencing Verfahrens.

Alexander Grenz: Aufbau eines Referenzfestpunktfeldes zum Betrieb eines Outdoor-Baumaschinensimulators.

Kauker, Stephanie: Untersuchung verschiedener Laserscanner-Zielzeichen für die Registrierung von Punktwolken.

Scatturin, Raphael: Barometrische Höhenbestimmungen in einem Hydrographischen Ortungssystem (HydrOs).

Schaal, Carolin: Untersuchung des Auflösungsvermögens eines Laserscanners bei der Aufnahme feiner Strukturen.

Tao, Qin: Genauigkeitsuntersuchung der Low-cost IMU 3DM-GX2 von Microstrain.

Wang, Jinyue: Neuvermessung des Pfeilernetzes Vaihingen und Vergleich mit Low-Cost GPS Ergebnissen.

Wilhelm, Johannes: Untersuchungen zur Modellierung und der Datenmigration von kommunalen Daten im Rahmen des Abwassergebührensplittings.

Yang, Jiawei: Erfassung von Spannungs- und Meteorologiedaten für das Low-Cost GPS Monitoring System.

Ye, Zican: Untersuchung der inneren und äußeren Genauigkeit des Faro Focus 3D.

Yue, Fang: Einsatz von koordinatenbasierten Verfahren zum Location Referencing.

8. Education

Bachelor Geodesy and Geoinformatics:

Basic Geodetic Field Work (Schmitt, Stange) 5 days

Engineering Geodesy in Construction Processes (Schwieger, Zheng) 3 Lecture/1 Lab

Geodetic Measurement Techniques I (Metzner, Schmitt) 3/1

Geodetic Measurement Techniques II (Schmitt) 0/1

Integrated Field Work (Metzner, Zheng) 10 days

Measurement Methods and Estimation Methods in Engineering Geodesy (Schwieger, Zheng) 2/2

Reorganisation of Rural Regions (Helfert) 1/0

Statistics and Error Theory (Schwieger, Zhang) 2/2

Master Geodesy and Geoinformatics:

Industrial Metrology (Schwieger, Stange, Schmitt) 1/1

Land Development (Meyer) 1/0/0/0

Monitoring Measurements (Schwieger, Lerke) 1/1

Transport Telematics (German) (Metzner, Scheider) 2/2

Thematic Cartography (German) (Beetz, Metzner, Schützle) 1/1

Terrestrial Multisensor Data Acquisition (German) (Beetz, Schmitt) 1/1

Measurement Techniques within Closed Loops (Beetz) 2/0

Project Management in Engineering Geodesy (Wiltschko, Völter) 2/0

Master GeoEngine:

Integrated Field Work (Metzner, Zheng) 10 days

Kinematic Measurements and Positioning (Schwieger, Beetz) 2/1

Thematic Cartography (Schützle) 1/1

Transport Telematics (Metzner, Scheider) 2/1

Monitoring (Schwieger, Lerke) 1/1

Bachelor "Civil Engineering":

Geodesy in Civil Engineering (Beetz, Scheider) 2/2

Master "Civil Engineering":

Geoinformation Systems (Metzner, Zheng) 2/1

Transport Telematics (Metzner, Scheider) 1/1

Bachelor "Technique and Economy of Real Estate"

Acquisition and Management of Planning Data (Metzner, Stange) 2/2

Master "Infrastructure Planning".

GIS-based Data Acquisition (Beetz, Schmitt) 1/1

Bachelor "Transport Engineering":

Statistics (Metzner, Stange) 0.5/0.5

Seminar Introduction in Transport Engineering (Metzner, Schmitt) 0.5/0.5